Acta Technica *61*, No. 4B/2016, 9–18

Vibration analysis of a shaft-bladed system by using solid models[1]

Chunlong Zheng[2], Xueshi Yao[2,3]

Abstract. To study the vibration characteristics of a rotating shaft-bladed system, the spin softening effect of finite element method (FEM) was incorporated with prestress effect to analyze the shaking, swing, torsion and their coupled vibration. The mathematical formula was derived from the Coriolis effects and gyroscopic inertia. The study shows that the centrifugal force exerts influence on the different order vibration frequencies. The effect of the spin softening has significant influence on the first order swing vibration frequency of the blades, but has little influence on the shaking and torsion vibration frequencies. With the variation of rotating velocity, the coupled vibration among shaking, swing and torsion could happen because their vibration frequencies change with the different magnitude of the increase. The coupled vibration is more destructive. The shaft's bending vibration split into forward whirl and backward whirl modes and the torsional vibration frequency does not change with the increase of the speed. The accuracy of the solid model and the solution techniques have been demonstrated by comparison with beam model results of a commercial software. The results further show the complexity of the dynamic characteristics of the shaft-bladed system. The work is helpful to improve the dynamic stability of the shaft-bladed system.

Key words. Shaft-bladed system, Coriolis effect, spin softening, swing vibration, coupled vibration..

1. Introduction

Resonant vibrations of a rotating shaft-bladed system can occur in many engineering structures such as aircraft propellers, helicopter and wind turbine rotors. To

[1]The authors are in debt to professors J. Chen and L. Q. Chen, Drs. T. Jia and W. H. Huang for their fruitful discussions. The work was supported by the Natural Science Foundation of China under Grant No. 11172181, the Natural Science Foundation of Guangdong Province of China under Grant No. 10151200501000008, the Educational Foundation of Scientific and Technical Innovation of Guangdong Province of China under Grant No. 2013KJCX0167, and the Scientific Research Foundation of Key Discipline of Guangdong Province of China.

[2]School of Physics and Electromechanical Engineering, Shaoguan University, Shaoguan 512005, China

[3]College of Mechanical and Electrical Engineering, Guangdong Baiyun University,Baiyun 510450, China

design the system, we must think of undergoing both global motion and longitudinal deformation. The coupling between the stress stiffness and deformation makes the dynamic characteristics of the system more complex, showing a strong nonlinearity. Due to the rotating speed over the critical speed, the system could have a destructive and non-synchronous whirl components because of the effects of Coriolis, variable load and deformation. Strong vibration will cause the accident, and bring about huge economic losses. In order to meet the engineering requirements, it is in an urgent need to improve the design level and optimize the shaft-bladed system.

Research on rotor dynamics is continually and steadily expanded in recent years. The coupled nonlinear equation which takes into account the stiffening effect is derived by applying the Lagrange equation for the moving beam, and based on the Newmark direct integration method and the Newton-Raphson iteration method, the computational procedures of the numerical method for solving the nonlinear equation are given [1].The influence of the curving and twisting of an elongated blade on its vibrations during complex rotation is studied, and it is shown that these geometrical factors may cause additional resonant vibrations [2].The blades are modeled as discrete multi-degree-of-freedom systems using the finite element software code ANSYS, and ANSYS is used to obtain the stiffness matrices of the blades, allowing the free vibration characteristics of the rotating blades to be determined by analytical formulation [3].The cylindrical rotor modes are not influenced by gyroscopic effects and remain at a fairly constant frequency versus rotor speed. Conversely, conical rotor modes are indeed influenced and caused to split into forward and backward whirl components that respectively increase and decrease in frequency with increased rotor speed [4]. Using solid models for the rotor dynamic analysis, the backward whirl is dominated by spin softening effect compared to the forward whirl frequencies where the stress stiffening plays a significant role [5–7].The study results on rotor dynamics provide a necessary foundation for further study on the shaft-bladed system [8–9].

2. Dynamic equation

2.1. *Dynamic equation of beam in rotating reference frame*

Using the rotating beam model to simulate a blade, the dynamic equation [8] is

$$[M]\{\ddot{u}_r\} + [C_{\mathrm{cor}}]\{\dot{u}_r\} + \{[K_{\mathrm{e}}]^{\mathrm{e}} + [K_{\mathrm{g}}]^{\mathrm{e}} + [K_{\mathrm{v}}]^{\mathrm{e}}\}\{u_r\} = \{F\}\ . \tag{1}$$

Here, $[M]$ is the mass matrix, $[C_{\mathrm{cor}}]$ denotes the Coriolis matrix, $[K_{\mathrm{e}}]^{\mathrm{e}}$ stands for the axial-lateral stiffness matrix of Euler-Bernoulli beam element model, $[K_{\mathrm{g}}]^{\mathrm{e}}$ represents the stiffness matrix of the centrifugal load corresponding to the angular velocity, $[K_{\mathrm{v}}]^{\mathrm{e}}$ is the spin softening stiffness matrix and F represents the load vector. Finally, symbol u_r stands for the vector of displacements.

The Coriolis matrix $[C_{\mathrm{cor}}]$ is given by the formula

$$[C_{\mathrm{cor}}] = 2\int_v \rho[N]^{\mathrm{T}}\varpi[N]\,\mathrm{d}v\,, \tag{2}$$

where $[N]$ is the shape function matrix,

$$[C_{\text{cor}}] = 2\int_v \rho[N]^{\text{T}}\varpi[N]\,\mathrm{d}v\,. \tag{3}$$

Here

$$\varpi = \begin{bmatrix} 0 & -\omega_z & \omega_y \\ \omega_z & 0 & -\omega_y \\ -\omega_y & \omega_z & 0 \end{bmatrix}, \tag{4}$$

where $\omega_x = \omega_y = 0$ and $\omega_z = \dot{\psi}$ is the rotating angular velocity ρ is the density and v is the volume of element. Finally,

$$u_r = [u_1, v_1, \beta_1, u_2, v_2, \beta_2]\ ,\quad (\beta_1, \beta_2) = (v_1', v_2')\ .$$

In our case

$$[C_{\text{cor}}] = \begin{bmatrix} 0 & \frac{-7}{10} & \frac{-1}{10} & 0 & \frac{-3}{10} & \frac{l}{15} \\ & 0 & 0 & \frac{3}{10} & 0 & 0 \\ & & 0 & \frac{l}{15} & 0 & 0 \\ & \text{antisym} & & 0 & \frac{-7}{10} & \frac{l}{10} \\ & & & & 0 & 0 \\ & & & & & 0 \end{bmatrix}, \tag{5}$$

Further,

$$[K_{\text{e}}]^{\text{e}} = \begin{bmatrix} A & 0 & 0 & -A & 0 & 0 \\ & \frac{12I}{l^2} & \frac{6I}{l} & 0 & -\frac{12I}{l^2} & \frac{6I}{l} \\ & & 4I & 0 & -\frac{6I}{l} & 2I \\ & & & A & 0 & 0 \\ & \text{sym} & & & \frac{12I}{l^2} & -\frac{6I}{l} \\ & & & & & 4I \end{bmatrix}, \tag{6}$$

$$[K_{\text{g}}]^{\text{e}} = \frac{EA}{60l^2}\begin{bmatrix} 0 & 0 & 0 & 0 & 0 & 0 \\ & 72\tilde{u} & 6\tilde{u}l & 0 & -72\tilde{u} & 6\tilde{u}l \\ & & 8\tilde{u}l^2 & 0 & -6\tilde{u}l & -2\tilde{u}l^2 \\ & & & 0 & 0 & 0 \\ & \text{sym} & & & 72\tilde{u} & -6\tilde{u}l \\ & & & & & 8\tilde{u}l^2 \end{bmatrix}, \tag{7}$$

where l is the beam element length and $\tilde{u} = u_2 - u_1$. The spin softening stiffness matrix is:

$$[K_{\text{v}}]^{\text{e}} = -\dot{\psi}^2\left([M_{\text{t}}]^{\text{e}} + [M_{\text{r}}]^{\text{e}}\right)\,, \tag{8}$$

where

$$[M_{\text{t}}]^{e} = \frac{\rho Al}{420}\begin{bmatrix} 140 & 0 & 0 & 70 & 0 & 0 \\ & 156 & 22l & 0 & 54 & -13l \\ & & 4l^2 & 0 & 13l & -3l^2 \\ & & & 140 & 0 & 0 \\ & \text{sym} & & & 156 & -22l \\ & & & & & 4l^2 \end{bmatrix}, \tag{9}$$

and

$$[M_{\mathrm{r}}]^e = \frac{\rho I}{l}\begin{bmatrix} 0 & 0 & 0 & 0 & 0 & 0 \\ & \frac{6}{5} & \frac{l}{10} & 0 & -\frac{6}{5} & \frac{l}{10} \\ & & \frac{2l^2}{15} & 0 & -\frac{l}{10} & -\frac{l^2}{30} \\ & & & 0 & 0 & 0 \\ & \text{sym} & & & \frac{6}{5} & -\frac{l}{10} \\ & & & & & \frac{2l^2}{15} \end{bmatrix}. \tag{10}$$

2.2. Dynamic equation of beam in stationary reference frame

Using the rotating beam model to simulate a shaft, the dynamic equation is

$$\{[M]_{\mathrm{t}} + [M]_{\mathrm{r}}\}\,\ddot{u} + [G]\dot{u} + [K]_{\mathrm{e}}u = F\,. \tag{11}$$

Here, $u^{\mathrm{T}} = [v_i, w_i, \theta_{iy}, \theta_{iz}, v_j, w_j, \theta_{jy}, \theta_{jz}]$, $[G]$ is the gyroscopic matrix, $[K]_{\mathrm{e}}$ is the elastic stiffness matrix and $\{u\}, \{\dot{u}\}, \{\ddot{u}\}$ are the displacement, velocity and acceleration vectors, respectively. The matrix $[G]$ may be expressed as

$$[G] = 2\int_0^l \rho I\,[N']^{\mathrm{T}}\,[\omega]\,[N']\,\mathrm{d}x = 2\int_0^l \rho I \begin{bmatrix} N_1' & 0 \\ 0 & N_1' \\ 0 & N_3' \\ N_3' & 0 \\ N_2' & 0 \\ 0 & N_2' \\ 0 & N_4' \\ N_4' & 0 \end{bmatrix}\cdot$$

$$\cdot\begin{bmatrix} 0 & -\dot{\psi} \\ \dot{\psi} & 0 \end{bmatrix}\cdot\begin{bmatrix} N_1' & 0 \\ 0 & N_1' \\ 0 & N_3' \\ N_3' & 0 \\ N_2' & 0 \\ 0 & N_2' \\ 0 & N_4' \\ N_4' & 0 \end{bmatrix}^{\mathrm{T}} \mathrm{d}x =$$

$$= 2\dot{\psi}\rho l \begin{bmatrix} 0 & \frac{6I}{5l^2} & -\frac{I}{10l} & 0 & 0 & -\frac{6I}{5l^2} & -\frac{I}{10l} & 0 \\ & 0 & 0 & -\frac{I}{10l} & \frac{6I}{5l^2} & 0 & 0 & -\frac{I}{10l} \\ & & 0 & \frac{2I}{15} & -\frac{I}{10l} & 0 & 0 & -\frac{I}{30} \\ & & & 0 & 0 & -\frac{I}{10l} & \frac{I}{30} & 0 \\ & & & & 0 & \frac{6I}{5l^2} & \frac{I}{10l} & 0 \\ & & & & & 0 & 0 & \frac{I}{10l} \\ & \text{antisym} & & & & & 0 & \frac{2I}{15} \\ & & & & & & & 0 \end{bmatrix}. \tag{12}$$

Symbols $M_{\mathrm{t}}, M_{\mathrm{r}}$ denote the translational and rotational inertial mass matrices and $\dot{\psi}$ is the angular velocity and $I = I_y = I_z$ is the bending moment of inertia. The one-dimensional beam models require good modeling techniques to approximate the three dimensional shaft. The effects of stress stiffening and spin softening are not included in the beam models as there is no cross-sectional dimension in the analysis. It is difficult to accurately obtain the calculation results in the rotor dynamics beam model.

2.3. Dynamic equations of solid in rotating reference frame

Using the solid model in rotating reference frame to simulate a blade, the dynamic equation is

$$[M]\{\ddot{u}_r\} + \{[C] + [C_{\mathrm{cor}}]\}\{\dot{u}_r\} + \Big\{[K] + [K_\sigma] - \dot{\psi}^2 [M]\Big\}\{u_r\} = \{F\}\,. \tag{13}$$

Here $[M]$ is the global mass matrix, $[C]$ is the global damping matrix, $[K]$ denotes the global stiffness matrix, $[K_\sigma]$ stands for the global prestress stiffening matrix and $-\Omega^2[M] = -\dot{\psi}^2[M]$ is the stiffness matrix corresponding to the spin softening.

Matrix $[K_\sigma]$ can be expressed as

$$[[K_\sigma] = \begin{bmatrix} S_0 & 0 & 0 \\ 0 & S_0 & 0 \\ 0 & 0 & S_0 \end{bmatrix}, \tag{14}$$

$$[S_0] = \int_v [S_{\mathrm{g}}]^{\mathrm{T}} [S_{\mathrm{m}}][S_{\mathrm{g}}]\,\mathrm{d}v\,, \quad [S_m] = \begin{bmatrix} \sigma_x & \sigma_{xy} & \sigma_{xz} \\ \sigma_{xy} & \sigma_y & \sigma_{yz} \\ \sigma_{xz} & \sigma_{yz} & \sigma_z \end{bmatrix} \tag{15}$$

and

$$[S_{\mathrm{g}}] = \begin{bmatrix} \frac{\partial N_1}{\partial x} & \frac{\partial N_2}{\partial x} & \dots & \frac{\partial N_8}{\partial x} \\ \frac{\partial N_1}{\partial y} & \frac{\partial N_2}{\partial y} & \dots & \frac{\partial N_8}{\partial y} \\ \frac{\partial N_1}{\partial z} & \frac{\partial N_2}{\partial z} & \dots & \frac{\partial N_8}{\partial z} \end{bmatrix}. \tag{16}$$

2.4. Dynamics equation of solid in stationary reference frame

Using the solid model in stationary reference frame to simulate a shaft, the dynamic equation is

$$[M]\{\ddot{u}\} + \{[C] + [G_{\mathrm{gyr}}]\}\{\dot{u}\} + \Big\{[K] + [K_\sigma] - \dot{\psi}^2 [M]\Big\}\{u\} = (F)\,. \tag{17}$$

The rotating shaft-bladed system to be modeled must be axisymmetric and the gyroscopic matrix generated is valid only for the linear analysis. The centrifugal effects of distributed shafts and mounted blades are included. Stress stiffening and spin softening are included, which have significant effect on the critical speeds and unbalance response. The rotor dynamics analysis can now predict the whirl amplitudes more accurately, rather than just estimating the critical speeds and unstable regimes, thus improving the design capabilities of the shaft-bladed system [6].By setting the effects of gyroscopes, prestress and spin softening, formula (17) ($\{f_{\mathrm{g}}\} = [G_{\mathrm{gyr}}]\,\{\dot{u}\}$ being the gyroscopic moment) could correctly complete the dynamic analysis of the rotating shaft-bladed system by using the solid model of Ansys version 10.0.

3. Numerical results

3.1. Illustrative example

A helicopter blade radius is 10 m (along y axis), its width is 0.23 m. The blade cross-sectional area does not change along the radius. Based on a single blade as an example, its cross-sectional model is depicted in Fig. 1 and particular points have the following coordinates:

$$1:\ (0,0,-0.14)\,,\quad 2:\ (0,0,0.06)\,,\quad 3:\ (0.0133,0,0.09)\,,$$
$$4:\ (0.03,0,0.05)\,,\quad 5:\ (0.0167,0,-0.04)\,.$$

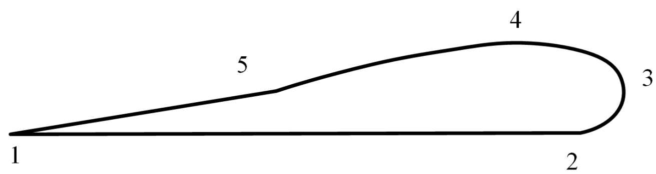

Fig. 1. Model of blade

The shaft length is 2.5 m with its outer diameter 0.06 m and inner diameter 0.04 m. The disk is placed in the axial direction of 1.74 m from the rotating blade center, of the disk thickness 0.08 m and diameter 0.4 m. The four blades are far from the disk, mounted on the outside of the bearing. Bearings of length 0.1 m are located on the center of shaft 0.1 m and 2.5 m. The actual shaft-bladed system is connected into a whole solid by the four blades and a shaft. The material performance parameter is

$$E = 42.6 \cdot 10^9\,\mathrm{Pa}\,,\ \mu = 0.28\,,\ \rho = 1950\,\mathrm{kg\,m^{-3}}\,.$$

3.2. Calculation results

On the platform of Ansys 10.0, the blade is discretized by a mesh with 6362 nodes and 6478 solid46 elements. Based on different rotating speed, the vibration model of the blades is calculated in the shaft-bladed system. The Campbell diagram is given in Fig, 2, and the first swing vibration model as shown in Fig. 3. The results show that the centrifugal force exerts influence on the different order vibration frequencies. Spin softening has great influence on the first swing frequency, but only a little influence on shaking and torsion vibration frequencies. With the variation of rotating velocity, the coupled vibration among shaking, swing and torsion can occur because their vibration frequencies change with the different magnitude of the increase. The coupled vibration is more destructive. The accuracy of the solid model and the solution techniques have been demonstrated by comparison with the beam element model.

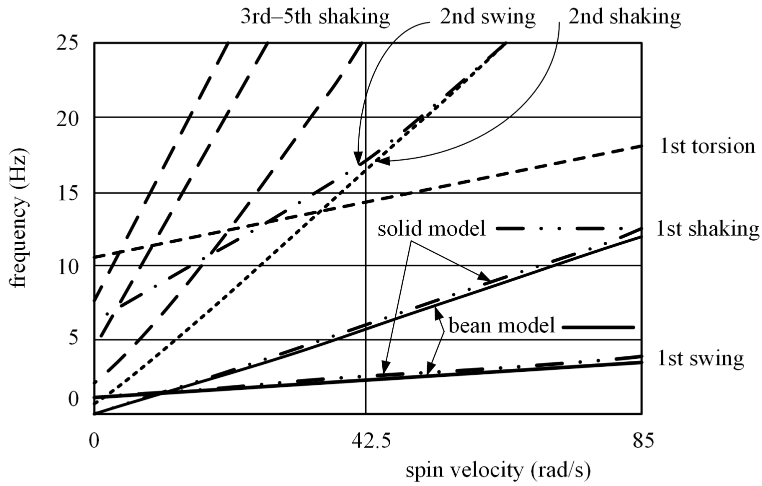

Fig. 2. Vibration model of blades

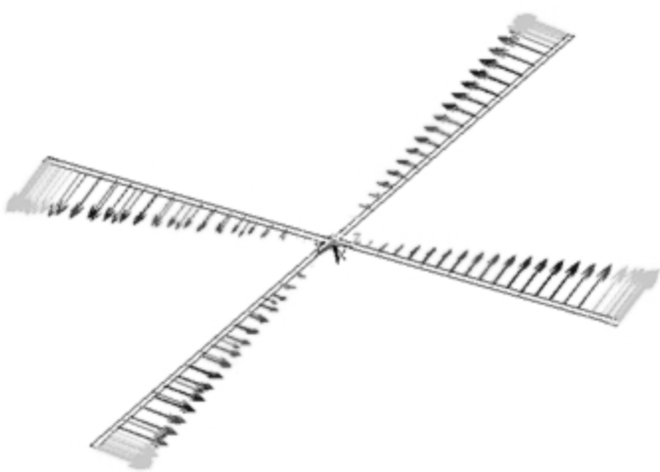

Fig. 3. First swing vibration

The shaft's Campbell diagram in the shaft-bladed system is given in Fig. 4. The vibration modes are compared between the solid and beam models. The bending vibration split into forward whirl mode and backward whirl mode.The bending vibration modes are related with the shaft structure. The torsional vibration frequency does not change with the increasing speed. The beam model of the shaft does not take account the stress stiffness and spin softening effects that play an important role in the solid model. The solid model rotor dynamics provides an accurate solution for such problems.

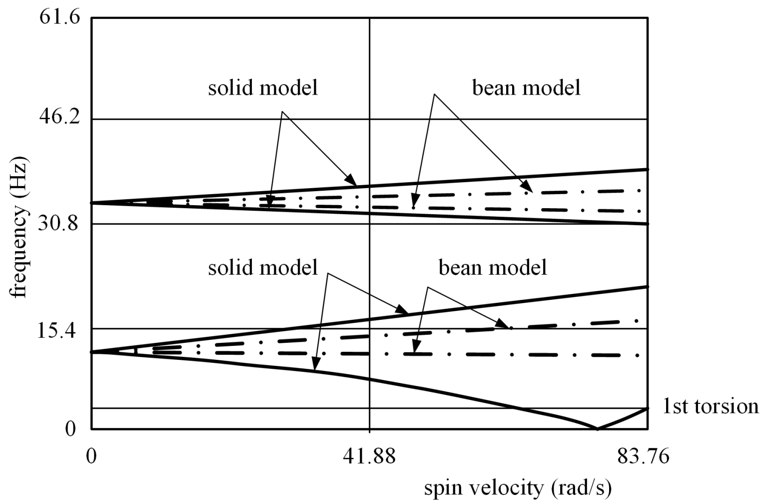

Fig. 4. Vibration model of shaft

The shaking, swing, torsion and their coupled vibration of the shaft-bladed system are calculated by solid and beam modes. The calculation shows that the spin softening has great influence on the first swing frequencies of the blades, but only a little influence on shaking and torsion vibration frequencies. The shaft bending vibration split into forward whirl mode and backward whirl mode and the torsional vibration frequency does not change with the increase of speed. The bending vibration models are related to the shaft structure. With the variation of rotating velocity, the coupled vibration between the blades and shaft can be induced easily.

A solid model shaft is used here, where centrifugal effects can play significant role in stress stiffening and spin softening effects, which are not considered in beam models. A specific advantage of the solid model lies in the fact that the whole model of the shaft-bladed system can be accounted in one analysis, which is impractical in beam models. Solid model rotor dynamics provides an accurate solution for such problems. The work lays a basic foundation for improving the dynamic stability of the shaft-bladed system.

4. Conclusion

Shaking, swing, torsion and coupled vibration of the shaft-bladed system are calculated by solid and beam modes. Calculation shows that the spin softening has great influence on the first swing frequencies of the blades, but has only a little influence on shaking and torsion vibration frequencies. The shaft bending vibration splits into forward whirl and backward whirl modes and torsional vibration frequency does not change with the increase of the speed. The bending vibration models are related to the shaft structure. With the variation of rotating velocity, the coupled vibration between the blades and shaft can be induced easily.

Solid model shaft is used here, where centrifugal effects can play significant role in stress stiffening and spin softening effects, which are not considered in the beam models. A specific advantage of the solid model lies in the fact that the whole model of the shaft-bladed system can be calculated in one analysis, which is impractical in the beam models. Solid model rotor dynamics provides an accurate solution for such problems. The work lays a basic foundation for improving the dynamic stability of the shaft-bladed system.

References

[1] A. Y. T. Leung, G. R. Wu, W. F. Zhong: *Vibration analysis of flexible beam undergoing both global motion and elastic deformation.* IJ Str. Stab. Dyn. *4* (2004), No. 4, 589–598.

[2] V. I. Gulyaev, S. N. Khudolii: *Vibrations of curved and twisted blades during complex rotation.* Int. App. Mech. *41* (2005), No. 4, 449–454.

[3] P. J. Murtagh, B. Basu, B. M. Broderick: *Mode acceleration approach for rotating wind turbine blades.* J Multi-body Dynam. *218* (2004), No. 3, 159–167.

[4] E. Swanson, C. D. Powell, S. Weissman: *A practical review of rotating machinery critical speeds and modes.* Sound and Vibration *39* (2005), No. 5, 10–17.

[5] J. S. Rao: *Rotor dynamics of aircraft gas turbine engines.* J Aerospace Sci. Technol. *60* (2008), No. 3, 169–182.

[6] J. S. Rao, R. Sreenivas: *Dynamics of a three level rotor system using solid elements.* Proc. IC Joint Power Generation, 16–19 June 2003, Atlanta, USA, pp. 601–606.

[7] X. S. Yao, C. L. Zheng, Y. F. Liao: *Dynamics of turbocharger rotor with spin softening effect.* Appl. Mechanics and Materials *397–400* (2014), 90–94.

[8] M. A. Trinidade, R. Sampaio: *Dynamics of beams undergoing large rotations accounting for arbitrary axial deformation.* J Guidance Control and Dynamics *25* (2002), No. 4, 634–643.

[9] Z. L. Mahri, M. S. Rouabah: *Calculation of dynamic stresses using finite element method and prediction of fatigue failure for wind turbine rotor.* WSEAS Trans. Appl. Theor. Mechanics *3* (2008), No. 1, 28–41.

Received November 16, 2016